

Structure-Activity Relationships of New Phytotoxic Metabolites with the Botryane Skeleton from *Botrytis cinerea*.

Rosa Durán-Patrón, Rosario Hernández-Galán, Laureana G. Rebordinos[‡],
Jesús M. Cantoral[‡] and Isidro G. Collado^{*}.

Departamento de Química Orgánica, Facultad de Ciencias, Universidad de Cádiz, Apdo. 40, 11510 Puerto Real, Cádiz, Spain.

[‡]Laboratorio de Genética y Microbiología, Facultad de Ciencias del Mar, Universidad de Cádiz, Apdo. 40, 11510 Puerto Real, Cádiz, Spain.

Received 8 October 1998; revised 22 December 1998; accepted 7 January 1999

Abstract

The fungal antibiotic botrydial (**1**) and related compounds constitute an important group of metabolites whose biological activity was not previously known in depth. The isolation, in addition to known compounds, of three new epimer metabolites with the botryane structure has allowed us to study the structure-activity relationships. The results suggest that, in addition to the presence of the dialdehyde functionality, the antibiotic, phytotoxic and cytostatic activities shown by some of these compounds are strongly correlated with the stereochemistry of the C-1/C-8 dialdehyde moieties. The relative configuration (*S*) of the C-1 substituent seems to play a critical role in the binding of the substrate to the chemoreceptor. © 1999 Elsevier Science Ltd. All rights reserved.

Keywords: *Botrytis cinerea*; metabolite; botryane; phytotoxic; cytotoxic; antibiotic; structure-activity.

INTRODUCTION

Most saturated and unsaturated dialdehydes possess potent bioactivities. They are, for instance, antibiotic,¹ fish toxic,² antifeedant³ and, in certain cases, have been suggested to be natural defence metabolites.³

It has been reported that the biological activities of these compounds are linked to the dialdehyde functionality.³ However, small structural changes may modulate the biological activities considerably, and the absolute stereochemistry of the dialdehydes, as well as their ability to form bioactive autooxidation products during a bioassay, has been suggested to be of importance.⁴

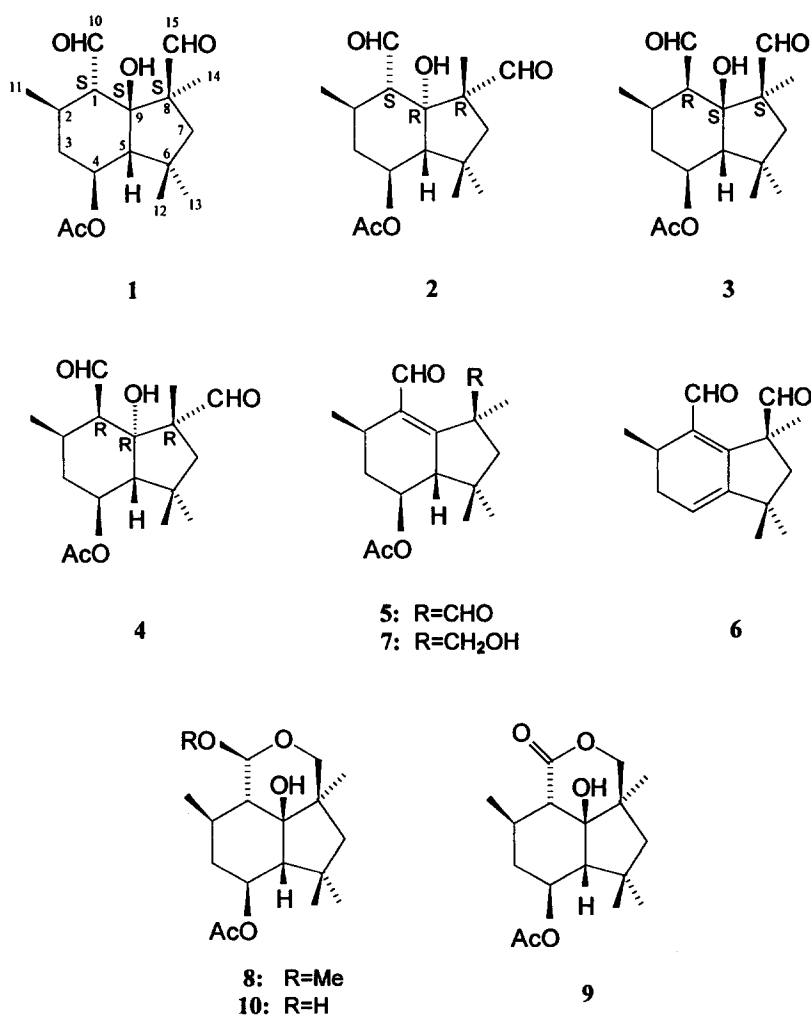
Botrydial⁵ (**1**) and structurally related compounds are characteristic metabolites of the phytopathogen *Botrytis cinerea*. These compounds possess a 1,5-dialdehyde functionality with

^{*} Author to whom correspondence should be addressed

which has been reported to be responsible of the bioactivity showed by this compounds.

Previous results obtained by our research group have shown that these metabolites are responsible for the typical necrotic lesion of the fungal infection and play an important role in the pathogenicity of the organism *in vivo*^{6,7}. In particular, botrydial (1) has shown phytotoxic activity on tobacco leaves at a concentration of only 1 ppm⁶. Likewise, this compound has also shown an interesting antibiotic activity against *Bacillus subtilis* and *Phytium debaryanum* at 400 and 100 ppm, respectively⁵.

During the course of our investigation into new metabolites from *B. cinerea*, we detected, in addition to other known metabolites, three new epimers of botrydial (1) from the strain *B. cinerea* 2100. The bioassays carried out allowed us to relate the structural changes with the potency of their biological activities.



RESULTS AND DISCUSSION

The strain *B. cinerea* 2100, obtained from CECT (Colección Española de Cultivos Tipo), was cultured by shaking on a Czapeck-Dox medium for 3 days. The fermentation broth was extracted with ethyl acetate as described in the Experimental section. Chromatography of the extract on silica gel, followed by final purification using HPLC (normal phase, petroleum ether/ethyl acetate), led to the isolation of 3 new epimers of botrydial (1): 8,9-epibotrydial (2), 1-epibotrydial (3) and 1,8,9-epibotrydial (4). Furthermore, metabolites 1⁵ and 5–10^{5,7-10} were isolated in sufficient amounts to allow the phytotoxic, antibiotic and cytotoxic assay.

Compound 2 was obtained as a crystalline material, the high-resolution mass spectrum, of which indicated a molecular formula C₁₇H₂₆O₅. Its ¹H-NMR spectrum (see Table 1) showed signals very similar to those of botrydial (1). However, the upfield shift of the signals corresponding to H-5 and H-1 and the deshielding of the signals corresponding to H-2, H-4, H-13 and H-14 suggested that this compound was the C-8, C-9 epimer of botrydial (1). In addition, the signal to $\delta = 3.71$ ppm assigned to the hydroxyl group appeared as a doublet by a long distance coupling with H-5, as showed the COSY experiment. This fact confirmed a R configuration for C-9. A qualitative analysis of the N.O.E. experiments confirmed this. In particular, N.O.E. interactions were detected between H-5, H-1 and H-14, supporting the proposed stereochemistry of the aldehyde group at C-8. Likewise, N.O.E. interactions were observed between H-15, H-10, H-2, H-4 and C₉-OH, confirming the epimerization at C-9 (see Figure 1).

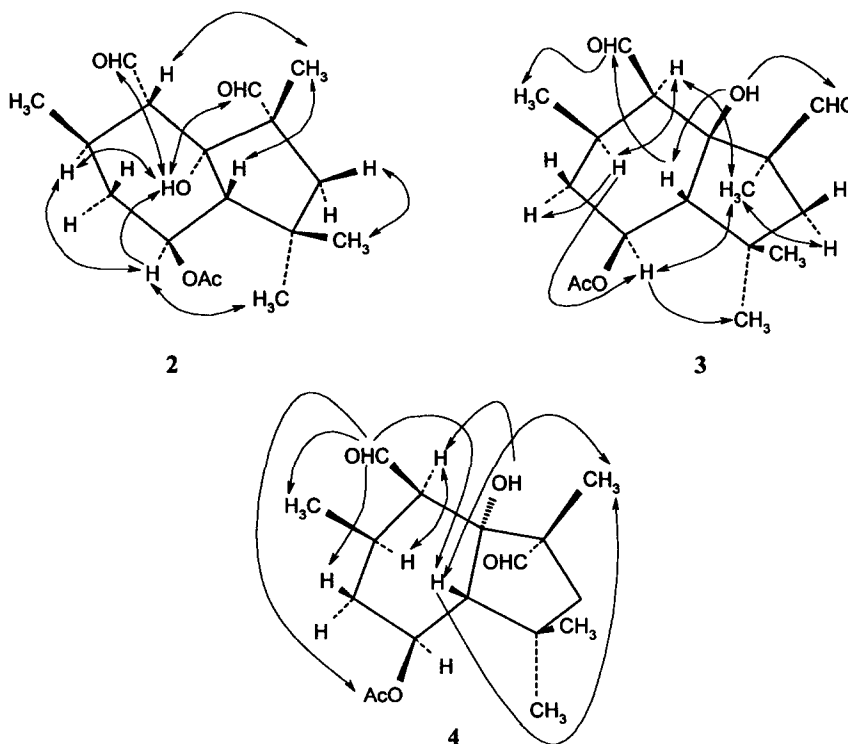


Figure 1. Selected N.O.E. correlations observed in compounds 2, 3 and 4.

Table 1. 400 MHz ^1H -NMR data of compounds 2, 3 and 4 in CDCl_3 .

Proton	2	3	4
1	2.15 (dd)	2.85 (dd)	2.73 (t)
2	2.49 (m)	2.23 (m)	2.59 (m)
3 α	2.26 (ddd)	1.99 (ddd)	2.11 (ddd)
3 β	1.00 (ddd)	1.54 (ddd)	1.40 (ddd)
4	5.26 (ddd)	4.98 (ddd)	5.31 (ddd)
5	1.79 (dd)	2.15 (d)	2.43 (dd)
7 α	2.26 (d)	1.36 (d)	2.26 (d)
7 β	1.45 (d)	2.36 (d)	1.49 (d)
10	9.73 (d)	9.89 (d)	9.99 (d)
11	0.97 (d)	1.12 (d)	0.92 (d)
12	1.20 (s)	1.27 (s)	1.13 (s)
13	1.12 (s)	1.12 (s)	1.12 (s)
14	1.31 (s)	1.06 (s)	1.25 (s)
15	9.58 (s)	9.62 (s)	9.52 (s)
CH ₃ -COO	2.03 (s)	2.04 (s)	2.05 (s)
OH	3.71 (d)	3.63 (brs)	3.16 (d)

J (Hz): 2: $J_{1-2} = 11.2$; $J_{1-10} = 3.7$; $J_{3\alpha-3\beta} = 12.5$; $J_{3\alpha-4} = 4.7$; $J_{3\beta-4} = 11.0$; $J_{4-5} = 11.0$; $J_{5-\text{OH}} = 1.6$; $J_{7\alpha-7\beta} = 13.3$; $J_{11-2} = 6.6$. 3: $J_{1-2} = 5.9$; $J_{1-10} = 3.3$; $J_{3\alpha-2} = 4.5$; $J_{3\alpha-3\beta} = 13.4$; $J_{3\alpha-4} = 4.6$; $J_{3\beta-2} = 9.8$; $J_{3\beta-4} = 8.4$; $J_{4-5} = 8.4$; $J_{7\alpha-7\beta} = 13.6$; $J_{11-2} = 7.3$. 4: $J_{1-10} = 5.3$; $J_{3\alpha-2} = 4.2$; $J_{3\alpha-3\beta} = 13.2$; $J_{3\alpha-4} = 5.2$; $J_{3\beta-2} = 13.2$; $J_{3\beta-4} = 10.8$; $J_{4-5} = 10.8$; $J_{5-\text{OH}} = 1.8$; $J_{7\alpha-7\beta} = 12.9$; $J_{11-2} = 7.3$.

Table 2. 50 MHz and 100 MHz ^{13}C -NMR data of compounds 2, 3 and 4 in CDCl_3 .

Carbon	2 (50MHz)	3 (100MHz)	4 (100MHz)
1	60.34 (d)	55.61 (d)	^a 53.27 (d)
2	29.13 (d)	29.52 (d)	30.34 (d)
3	40.20 (t)	34.11 (t)	36.22 (t)
4	70.64 (d)	71.34 (d)	71.54 (d)
5	58.28 (d)	60.88 (d)	^a 60.24 (d)
6	38.21 (s)	38.77 (s)	37.60 (s)
7	50.87 (t)	48.92 (t)	50.33 (t)
8	57.16 (s)	59.63 (s)	58.69 (s)
9	89.19 (s)	86.86 (s)	86.88 (s)
10	207.52 (d)	205.50 (d)	204.31 (d)
11	19.47 (q)	19.46 (q)	^b 21.00 (q)
12	34.25 (q)	34.52 (q)	34.54 (q)
13	27.06 (q)	28.01 (q)	27.58 (q)
14	19.25 (q)	18.79 (q)	^b 18.25 (q)
15	207.79 (d)	205.79 (d)	206.43 (d)
CH ₃ -COO	21.28 (q)	21.51 (q)	21.29 (q)
CH ₃ -C=O	170.26 (s)	170.17 (s)	-

^{a, b} = interchangeable signals.

Compound **3** is also a crystalline material and possesses a molecular formula $C_{17}H_{26}O_5$ and hence it is isomeric with botrydial (**1**). Although the 1H - and ^{13}C -NMR spectra (see Tables 1 and 2) are similar to those of botrydial (**1**), the chemical shifts of H-1, H-3 β , H-3 α , H-5 and H-11 are different, while the magnitude of the coupling constant $J_{1,2}$ was found to change from 12.2 Hz in botrydial (**1**) to 5.9 Hz in **3**. Hence, this compound was confirmed as the C-1 epimer of botrydial (**1**). N.O.E. experiments confirmed the stereochemistry of the aldehyde group at C-1. In particular, irradiation of the H-1 signal caused enhancement of the H-2 and H-14 signals, while irradiation of the H-2 signal produced enhancement of the H-1, H-4 and H-3 α signals, and irradiation of the H-14 enhanced the H-1, H-4 and H-7 α signals. Irradiation of the H-10 signal caused enhancement of the signals of H-3 β and H-11, while irradiation of the H-5 and C₉-OH signals enhanced the H-10 signal. These enhancements support the proposed structure and stereochemistry for 1-epibotrydial (**3**) (see Figure 1).

The high-resolution mass spectrum and ^{13}C -NMR spectrum (17 signals) (see Table 2) of compound **4** established the molecular composition as $C_{17}H_{26}O_5$. Hence, this compound is another isomer of botrydial (**1**). The 1H -NMR spectrum of this compound (see Table 1) showed very similar signals to those of botrydial (**1**). The principal difference observed between the two spectra involves the form of the H-1 signal, which had changed from *dd* in botrydial (**1**) to *t* in **4**, indicating an epimerization at C-1. This inference was supported by a deshielding of the signals corresponding to H-1, H-3 β and H-5. Likewise, the presence of the signal corresponding to the hydroxyl group as a doublet by the long distance coupling with H-5 suggested a change in the stereochemistry at C-9. This was confirmed by N.O.E. experiments. In particular, irradiation of the H-10 signal caused enhancement of the H-3 β , H-5, H-11 and CH₃COO signals, while irradiation of the H-1 signal enhanced the signal corresponding to H-2. Likewise, N.O.E. interactions were found between C₉-OH and H-1, and between H-5 and H-14 (see Figure 1). Hence, this compound is the C-1, C-8, C-9 epimer of botrydial (**1**).

In order to relate the structural changes with the bioactivity, compounds **2–9** were tested as phytotoxics and compounds **1–4** and **6–9** as antibiotics. In addition, botrydial (**1**) and dihydrobotrydial (**10**), the major metabolites from the fungus, were tested as cytotoxics.

Phytotoxicity assays were carried out using the methodology described in the Experimental section. Solutions of the metabolites (**2–9**) were prepared by dissolving the material in acetone and adding water that contained 0.1% Tween 80, to yield concentrations of 1000, 500, 250, 100, 50, 25 and 10 ppm. The final volume of acetone in each case was 40%. The solutions were placed on 1 cm¹ diameter circles of tobacco leaves and the leaves were then incubated for a further period. The results showed that compounds **7**, **8** and **9** were inactive while compounds **2–6** displayed phytotoxic activity. The results are summarised in Table 3.

The activities shown by epimer derivatives **2–4** are quite diverse. The difference between botrydial (**1**) and its epimers is dramatic. Compound **1** showed high activity at a concentration of 30 ppm, with the least effective concentration being 1 ppm,⁶ while the 8,9-epimer derivative (**2**) was active at 100 ppm, and compounds **3** and **4** displayed a minimal effective concentration at 250 and 750 ppm, respectively. Clearly, the configuration (*S*) at the C-1 substituent plays a critical role by interacting with approaching nucleophiles and, consequently, may be important for binding of the substrate to the receptor site.³

Table 3. Phytotoxic effect on *Nicotiana tabacum* of compounds 2–6 on day 7 of the bioassay.

Metabolite concentration (ppm)	% Affected circles*	% Affected surface**
8,9-Epibotrydial (2)		
1000	100	23.6
500	62	22.2
250	89	17.5
200	82	12.8
100	51	8.8
1-Epibotrydial (3)		
1000	100	18.8
500	96	14.1
250	10	0.4
1,8,9-Epibotrydial (4)		
1000	52	4.4
750	22	0.4
Botryendial (5)		
1000	100	64.3
500	94	49.6
250	94	49.0
125	93	30.1
50	48	1.3
25	5	0.1
Botrydienal (6)		
1000	100	83.5
500	98	58.5
250	100	45.4
100	100	14.9
50	74	10.4
20	74	9.8

*Arithmetic mean of the results from two independent experiments with 25 circles for each concentration in each experiment (Standard deviation was always lower than 3%).

**Calculated as the surface affected compared to the total surface expressed in mm².

Interestingly, the unsaturated dialdehydes **5** and **6** were more active than epimers **2–4** and slightly less active than botrydial (**1**). Botryendial (**5**) and botrydienal (**6**) showed a high activity at concentrations of 125 and 20 ppm, respectively, with the minimal effective concentration (MEC) being 25 ppm (**5**) and 10 ppm (**6**). It is worth noting that these compounds were active after only 24 h at all concentrations bioassayed. In addition, compound **5** reproduced the characteristic necrotic zone of the plant disease. It is important to note that botrydial (**1**) is easily transformed into derivatives **5** and **6** upon treatment with oxalic acid,⁷ and quantitatively transformed into **6** upon treatment with Fetizon's reagent.¹¹

On the other hand, when dialdehyde **1** was oxidised to the diacid (see Experimental section), the corresponding dimethyl ester was found to be inactive. Another methyl ester derivatives of botrydial (**1**) have been described as non-phytotoxic.⁷

Table 4. Antibiotic activity of compounds **1**, **2** and **6** against *Bacillus subtilis*.

Metabolite concentration (ppm)	Diameter of inhibition zones (mm)
Botrydial (1)	
500	20
250	18
100	13
8,9-Epibotrydial (2)	
500	25
250	16
150	13
Botrydienal (6)	
500	18
400	13

As described above, it had been reported that botrydial (**1**) shows an interesting antibiotic activity while dihydrobotrydial (**10**) is inactive. This fact seems to be related with the structural changes of these compounds. To confirm these data, compounds **1–4** and **6–9** were tested against *Bacillus subtilis* following the methodology described in the Experimental section. Compounds **1**, **2** and **6** were active with a minimum inhibitory concentration of 100, 150 and 400 ppm, respectively, while **3**, **4** and **7–9** were not active. The results are summarised in Table 4. Curiously, there is correlation between phytotoxic and antibiotic activities, as demonstrated by the fact that compounds **1**, **2** and **6** are more active as phytotoxic and antibiotic agents.

Table 5. Cytotoxicity assays of compounds **1** and **10** against tumoural and non-tumoural human cells.

Cellular lines	ID ₅₀ (µg/ml)	
	1	10
HUVEC	0.12	100
ASJ-4	1	— [#]
MDA-MB-231	5	—
HT-1080	5	—
HT-29	3	40

[#]not active below 100 µg/ml

On the other hand, botrydial (**1**) and dihydrobotrydial (**10**), the major metabolites isolated from the fungus, were tested as cytotoxics. Botrydial (**1**) showed high activity in screens to detect *in vitro* cytotoxicity against HUVEC endothelial cells of the umbilical cord, ASJ-4 prepuce fibroblast, MDA-MB-231 breast adenocarcinoma, HT-1080 fibrosarcoma, and HT-29 colon adenocarcinoma. The ID₅₀ values are summarised in Table 5. The results show that botrydial (**1**) is active to ID₅₀ values equal to or lower than 5 µg/ml against tumoural cells, but it is also highly cytotoxic against non-tumoural cells. However, compound **10** was not active

against human cellular lines ASJ-4, HT-1080 and MDA-MB-231 in concentrations below 100 $\mu\text{g/ml}$, and was cytotoxic for the more sensitive lines HT-29 ($\text{ID}_{50} = 40 \mu\text{g/ml}$) and HUVEC below 100 $\mu\text{g/ml}$.

It has been suggested that α,β -unsaturated aldehydes react as Michael acceptors with approaching nucleophiles, such as thiol or amine groups of proteins, while 1,4-dialdehyde moieties may form pyrrole derivatives with primary amino groups.⁴ Such pyrrole formation has only been observed for molecules that have the appropriate stereochemical configuration to allow intramolecular cyclization.¹²

A study using molecular models and molecular mechanical calculations¹³ revealed that compounds 1 and 2, which showed the highest activities, presented a similar spatial disposition of carbonyl groups. In these compounds the aldehyde groups are parallel where the aldehydic groups and the oxygen of the tertiary hydroxyl groups must be coplanar, as shown in Figure 2.

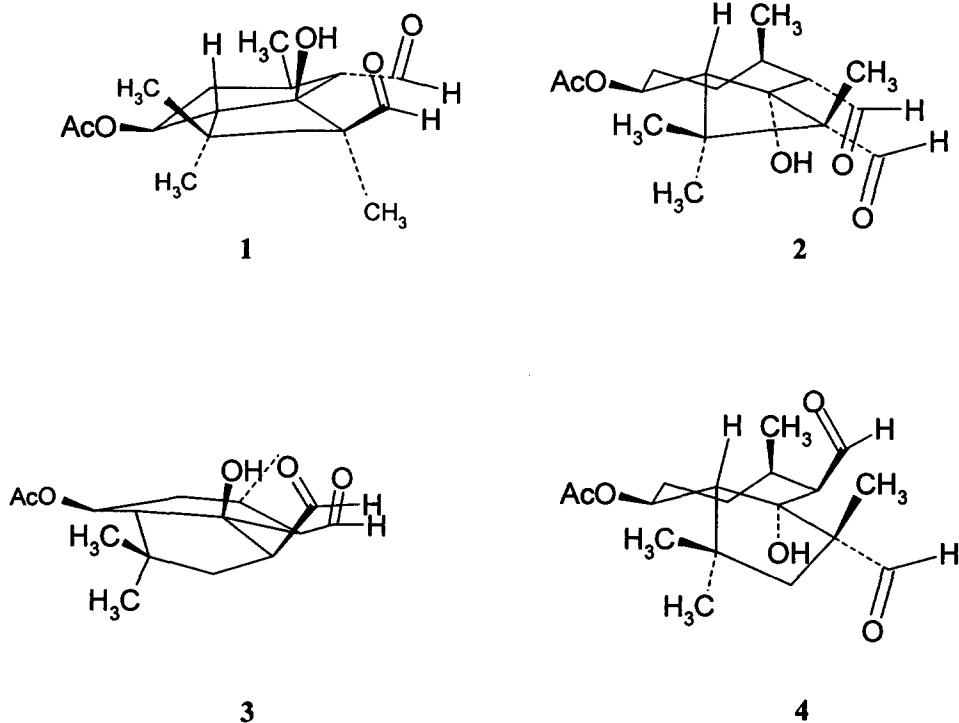


Figure 2. Comparison of the spatial arrangement of carbonyl and hydroxyl groups in compounds 1–4.

It can therefore be concluded that both corresponding carbonyl moieties at the C-1 and C-8 carbon atoms of botrydial and related derivatives should be in close enough proximity to allow intramolecular cyclization with thiol or amine groups of a chemoreceptor.

Clearly, the results described above show that the biological activities are correlated with the oxidation state of the aldehyde substituents at the C-1 and C-8 carbon atoms. This is especially apparent when comparing the structural differences between botrydial (**1**) and the analogous compounds **7–10**, including the methyl ester derivatives previously reported⁷.

Curiously, compounds **5** and **6**, which are unsaturated aldehydes that have been suggested to react as Michael acceptors^{4,14}, are less active than saturated aldehyde **1**, although they are more active than epimers **2–4**.

Differences in the biological activities of compounds **1** and **4** support the idea that bioactivity is strongly correlated with the stereochemistry of substituents at the C-1, C-8 and C-9 carbon atoms. In particular, the relative configuration (*S*) of the C-1 substituent seems to play a critical role in the binding of the substrate to the chemoreceptor.

EXPERIMENTAL

1.- General Methods

Melting points were determined with a Reichert-Jung Kofler block and are uncorrected. Optical rotations were determined with a Perkin-Elmer 241 polarimeter. IR spectra were recorded on a Perkin-Elmer 881 spectrophotometer. ¹H- and ¹³C-NMR measurements were obtained on Varian Gemini 200 and Varian Unity 400 NMR spectrometers with SiMe₄ as the internal reference. Mass spectra were recorded on VG 12-250 and VG-Autospec spectrometers at 70 eV. HPLC was performed with a Hitachi/Merck L-6270 apparatus equipped with a UV-VIS detector (L 4250) and a differential refractometer detector (RI-71). TLC was performed on Merck Kiesegel 60 F₂₅₄, 0.25 mm layer thickness. Silica gel (Merck) was used for column chromatography. Purification by HPLC was accomplished using a silica gel column (LiChrospher Si-60, 10 μm, 1 cm wide, 25 cm long or 5 μm, 0.4 cm wide, 25 cm long).

2.- Organism and Culture Conditions

Botrytis cinerea was obtained from the Colección Española de Cultivos Tipo (CECT), Facultad de Biología, Universidad de Valencia, Spain. The fungus was grown at 24–26 °C in 40 flasks (500 ml) containing 160 ml of Czapeck-Dox medium, per flask, of composition: 5% glucose, 0.1% yeast extract, 0.05% KH₂PO₄, 0.2% NaNO₃, 0.05% MgSO₄·7H₂O and 0.001% FeSO₄·H₂O. The pH of the medium was adjusted to 7.0 and each flask was inoculated with 40 ml of a suspension of a 48 h old culture. Cultures were incubated for 3 days on an orbital shaker at 250 rpm.

3.- Extraction and Isolation

The broth (8 l) was acidified to pH 2.0 with HCl, saturated with NaCl and extracted with EtOAc. The EtOAc extract was washed with NaHCO₃ and H₂O and dried over anhydrous Na₂SO₄. Evaporation of the solvent at reduced pressure gave a yellow oil that was separated by column chromatography on silica gel, with an increasing gradient of ethyl acetate in petroleum ether, followed by final purification using HPLC to afford botrydial⁵ (1) (587 mg), 8,9-epibotrydial (2) (10 mg), 1-epibotrydial (3) (41 mg), 1,8,9-epibotrydial (4) (2 mg), botryendial⁷ (5) (120 mg), botrydienal⁸ (6) (7 mg), botryenalol⁷ (7) (16 mg), *O*-methyl-dihydrobotrydial⁹ (8) (37 mg), 10-oxodihydrobotrydial¹⁰ (9) (3 mg) and dihydrobotrydial⁵ (10) (716 mg).

8,9-Epibotrydial (2)

White solid, mp 118–120 °C. $[\alpha]_D^{25} +34.7$ ($c = 0.24$, EtOAc). IR (film, CHCl₃) 3494, 2963, 2930, 2751, 1727, 1462, 1385, 1242, 1066 cm⁻¹. EIMS m/z (rel. int.) 311 [M + 1]⁺ (0.2), 293 [M + 1 - H₂O]⁺ (15), 251 [M + 1 - AcOH]⁺ (24), 233 [M + 1 - AcOH - H₂O]⁺ (26), 205 (51), 179 (65), 119 (100). HREIMS calcd. for C₁₇H₂₅O₄ [M + 1 - H₂O]⁺ 293.1753, found 293.1774. For ¹H- and ¹³C-NMR data see Tables 1 and 2.

1-Epibotrydial (3)

White solid, mp 109–111 °C. $[\alpha]_D^{25} +52.1$ ($c = 0.14$, CDCl₃). IR (film, CHCl₃) 3481, 2961, 2876, 2739, 1726, 1462, 1368, 1244, 1023 cm⁻¹. EIMS m/z (rel. int.) 310 [M]⁺ (4), 250 [M - AcOH]⁺ (4), 235 [M - AcOH - CH₃]⁺ (9), 204 (39), 175 (100). HREIMS calcd. for C₁₇H₂₆O₅ [M]⁺ 310.1780, found 310.1790. For ¹H- and ¹³C-NMR data see Tables 1 and 2.

1,8,9-epibotrydial (4)

Amorphous powder. $[\alpha]_D^{25} +38$ ($c = 0.16$, EtOAc). IR (film, CHCl₃) 3482, 2960, 2930, 2872, 2721, 1725, 1467, 1387, 1250, 1032 cm⁻¹. EIMS m/z (rel. int.) 250 [M - AcOH]⁺ (3), 232 [M - HOAc - H₂O]⁺ (1), 204 (16), 69 (32), 55 (32), 43 (100). HREIMS calcd. for C₁₇H₂₆O₅ [M]⁺ 310.1780, found 310.17655. For ¹H- and ¹³C-NMR data see Tables 1 and 2.

4.- Biological Assays

4.1.- Phytotoxicity assays

Tobacco leaves from *Nicotiana tabacum* var. Xanthi NC were used. The leaves were sterilised with 10% EtOH for 3 min, washed (x4) with sterile H₂O, dried between filter papers, cut into circles of 1 cm diameter and placed in Petri dishes (25 circles per plate) containing Whatman paper n° 1 wetted with sterile H₂O. The extract (10 µl) was placed on each of the circles and the plates were kept at 25–28 °C for 7 days.

The purified metabolites were dissolved in Me₂CO and 0.01% aq. Tween 80. The final volume of acetone in each case was 40% (v/v). Controls consisted of the same mixtures of Me₂CO-H₂O-Tween 80 as used for dissolving the purified metabolites.

Assays were carried out in duplicate and, for each concentration and product, two plates with the number of circles described above were obtained.

The results were obtained by counting the number of circles affected compared with the total (qualitative results) and by determining the surface area affected compared with the total surface area (quantitative results).

4.2.- Antibiotic assays

Petri dishes (9 cm diameter) containing TSA medium (1.6% peptone from casein, 0.3% peptone from soya, 0.25% glucose, 0.6% NaCl, 0.25% K₂HPO₄ and 1% agar, pH adjusted to 7.0) were inoculated with 3% of a culture of *B. subtilis* of OD₆₀₀ = 1. After solidification, cups were scooped out with a 10 mm sterile cork-borer and to each cup, 100 µl of a solution containing the test compound at the defined concentration was applied.

The solutions of the compounds were prepared using the methodology described above for the phytotoxicity assays. The same mixtures of Me₂CO/H₂O/Tween 80 were used as controls. The plates were kept at 4 °C for 2 h to permit the diffusion of the product and then incubated at 30 °C for 16 h. After this period, the diameter of inhibition zones was measured.

4.3.- Cytotoxicity assays

The cytotoxicity of the compounds was tested against tumoural and non tumoural human cells. The tumoural cellular lines used were MDA-MB-231 breast adenocarcinoma, HT-1080 fibrosarcoma and HT-29 colon adenocarcinoma, and the non tumoural cellular lines were HUVEC endothelial cells of the umbilical cord and ASJ-4 prepuce fibroblast.

The test compounds were dissolved in DMSO, carrying out consecutive solutions. Controls consisted of the same volume and identical dissolution of DMSO. The quantification was performed through incubation with MTT and reading of the absorbance at 550 nm. The measurements were duplicated.

5.- Oxidation of botrydial (1)

A solution of compound 1 (10 mg, 0.034 mmol) in 2 ml of EtOAc was treated with a solution of 8 mg of KMnO₄ in 150 µl of water and stirred vigorously for 3.5 h at room temperature. Excess reagent was then destroyed with Na₂SO₃. The reaction mixture was diluted with water, acidified to pH 2 and extracted with EtOAc (x4). The solvent was evaporated to give a gum, which was methylated with diazomethane. 1 ml of a solution of diazomethane (64–69% w/v) in diethyl ether were and mixture was stirred for 10 minutes. The solvent and excess of diazomethane were evaporated to afford 13 mg of dimethyl botrydiate (quantitative): mp 125, lit¹⁵ 125–126°C (Found: C, 61.8; H, 8.1. C₁₉H₃₀O₇ requires C, 61.6, 8.2%); IR(film, CHCl₃) 3435, 1730, 1700 cm⁻¹; ¹H-NMR (400 MHz, CDCl₃) 0.84 (3H, d, J=6.3, H-11), 1.08 (3H, s, H-13), 1.27 (3H, s, H-12), 1.53 (3H, s, H-14), 1.53 (1H, d, J= 12.5, H-7α), 1.97 (1H, d, J=11.3, H-5), 2.01 (1H, m, H-2), 2.03 (3H, s, CH₃COO-), 2.15 (1H, ddd, J= 3.0, 12.5, 11.3, H-3α), 2.28 (1H, d, J=12.5, H-7β), 2.55 (1H, d, J=12.6, H-1), 3.62, 3.65 (each 3H, s, -COOCH₃), 5.10 (1H, dt, J= 5.2, 11.3, H-4); ¹³C-NMR (100 MHz, CDCl₃) 20.2 (q, C-11), 21.3 (q, C-14), 21.4 (q, CH₃COO-), 27.4 (q, C-13), 30.0 (d, C-2), 35.6 (q, C-12), 37.8 (t, C-3), 38.4 (s, C-6),

51.5 and 52.0 (each q, -COOCH₃), 55.0 (s, C-8), 55.1 (t, C-7), 60.6 (d, C-5), 61.7 (d, C-1), 73.1 (d, C-4), 87.5 (s, C-9), 170.3 (s, CH₃COO-), 174.1 and 179.0 (each q, -COOCH₃).

ACKNOWLEDGEMENTS

This work was financed, in part, by grants from CICYT, PB95-1235-C-02-01 and FAIR 5-PL97-3351. Authors acknowledge Dr. H. H. Riese of the Company Antibióticos Farma for the undertaking of the bioassays of cytotoxic activity and to Dr. A. J. Macías-Sánchez (Departamento de Química Orgánica, Universidad de Cádiz) for the study carried out by molecular mechanical calculations.

REFERENCES

- [1] Anke H and Sterner O. *Planta Medica* **1991**; *57*: 344–346.
- [2] Asakawa Y, Harrison LJ and Toyota M. *Phytochemistry* **1985**; *24*: 261–262.
- [3] Fritz G, Mills G, Warthen J and Waters R. *J. Chem. Ecol.* **1989**; *15*: 2607–2623 and literature cited therein.
- [4] Jonassohn M, Anke H, Morales P and Sterner O. *Acta Chem. Scand.* **1995**; *49*: 530–535.
- [5] Fehlhäber HW, Geipel R, Mercker HJ, Tschesche R and Welmar K. *Chem. Ber.* **1974**; *107*: 1720–1730.
- [6] Rebordinos L, Cantoral JM, Prieto MV, Hanson JR and Collado IG. *Phytochemistry*. **1996**; *42*: 383–387.
- [7] Collado IG, Hernández-Galán R, Prieto V, Hanson JR and Rebordinos LG. *Phytochemistry*. **1996**; *41*: 513–517.
- [8] Kimata T, Natsume M and Marumo S. *Tetrahedron Lett.* **1985**; *26*: 2097–2100.
- [9] Kimura Y, Fujioka H, Nakajima H, Hamasaki T and Isogai A. *Agric. Biol. Chem.* **1988**; *52*: 1845–1847.
- [10] Collado IG, Hernández-Galán R, Durán-Patrón R and Cantoral JM. *Phytochemistry*. **1995**; *38*: 647–650.
- [11] Fetizon M, Golfier M and Louis J-M. *Tetrahedron* **1975**; *31*: 171–176.
- [12] Sodano G, Cimino G and Spinella A. *Tetrahedron Lett.* **1984**; *25*: 4151–4152.
- [13] Burkert U and Allinger NL. *Molecular Mechanics*, ACS Monograph 177, American Chemical Society, Washington, D.C., 1982.
- [14] Kubo I and Ganjian I. *Experientia* **1981**; *37*: 1063–1064.
- [15] Bradshaw PW and Hanson JR. *J. Chem. Soc., Perkin I* **1980**; 741–743.